ReGS: Reference-based Controllable Scene Stylization with Gaussian Splatting

Yiqun Mei*   Jiacong Xu*   Vishal M. Patel
Johns Hopkins University
{ymei7,jxu155, vpatel36}@jhu.edu

Abstract

Referenced-based scene stylization that edits the appearance based on a content-aligned reference image is an emerging research area. Starting with a pretrained neural radiance field (NeRF), existing methods typically learn a novel appearance that matches the given style. Despite their effectiveness, they inherently suffer from time-consuming volume rendering, and thus are impractical for many real-time applications. In this work, we propose ReGS, which adapts 3D Gaussian Splatting (3DGS) for reference-based stylization to enable real-time stylized view synthesis. Editing the appearance of a pretrained 3DGS is challenging as it uses *discrete* Gaussians as 3D representation, which tightly bind appearance with geometry. Simply optimizing the appearance as prior methods do is often insufficient for modeling continuous textures in the given reference image. To address this challenge, we propose a novel texture-guided control mechanism that adaptively adjusts local responsible Gaussians to a new geometric arrangement, serving for desired texture details. The proposed process is guided by texture clues for effective appearance editing, and regularized by scene depth for preserving original geometric structure. With these novel designs, we show ReGS can produce state-of-the-art stylization results that respect the reference texture while embracing real-time rendering speed for free-view navigation.

1   Introduction

Stylizing a 3D scene based on a 2D artwork is an active research area in both computer vision and graphics [1, 2, 3, 4, 5, 6, 7]. One important direction of stylization aims to precisely stylize the scene appearance based on a 2D content-aligned reference image drawn by users [10]. Such problem has numerous applications in digital art, film production and virtual reality. In the classical graphics pipeline, completing this task requires experienced 3D artists to manually create a UV texture map as input to the shader, a tedious process requiring professional knowledge, significant time, and effort.

Over the past decades, tremendous progress has been made in automatic scene stylization by leveraging view synthesis methods. While early attempts [1, 2, 12, 13] suffer from geometry errors of point clouds or meshes, more recent methods [9, 8, 3, 4, 5, 6, 7] rely on radiance field (NeRF) [14], a powerful implicit 3D representation, to deliver high-quality renditions that are perceptually similar to the reference image. A typical stylization workflow starts from a pretrained NeRF model of the target scene, followed by an appearance optimization phase to match the given style. The density function is always fixed to maintain the scene geometry [8, 9, 3, 10, 6] . Despite their promising results, NeRF-based approaches consume high training and rendering costs in order to obtain satisfactory results. Although some recent efforts make fast training possible [15, 16, 17, 18, 19, 20], the improvement in efficiency often comes at the price of degraded visual quality. Meanwhile, real-time rendering at inference time still remains challenging.

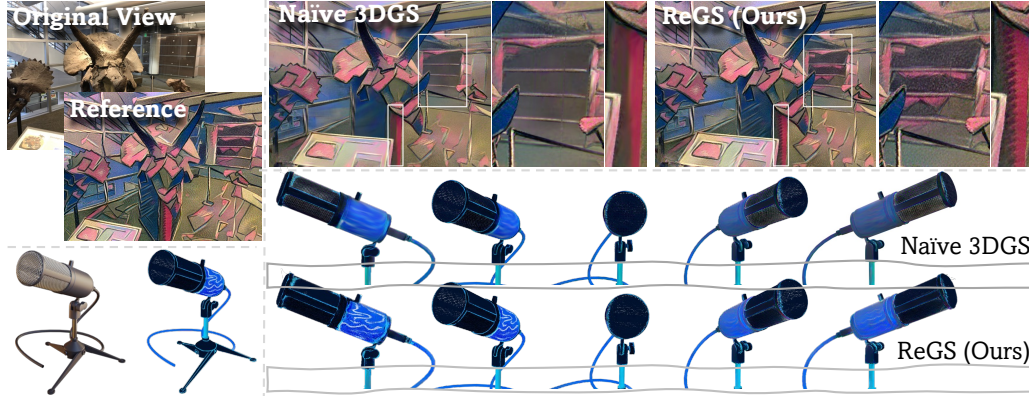*Equal contribution

Preprint. Under review.

Figure 1: Given a pretrained 3DGS model of the target scene and its paired style reference, ReGS enables real-time stylized view synthesis (at 134 FPS) with high-fidelity texture well-aligned with the reference. In contrast, only optimizing the appearance of 3DGS (denoted as Naive 3DGS), as previous methods [8, 9, 3, 10, 6] do, fails to capture many texture details in the reference. We tackle the challenges in high-fidelity appearance editing with a texture-guided control mechanism that is significantly more effective than the default density control [11] in addressing texture underfitting. Side-by-side comparisons with default density control can be found in Figure 5.

Recently, 3D Gaussian Splatting (3DGS) [11] has become an emerging choice for representing 3D scenes. 3DGS creates millions of colored Gaussians with learnable attributes to jointly represent the target scene geometry and appearance. Importantly, it adopts splatting-based rasterization [21] to replace the time-consuming volume rendering of NeRF models, providing remarkably faster rendering speed while maintaining comparable visual quality. However, as it uses *discrete* 3D Gaussians to represent the reconstructed scene, optimizing their appearance with a fixed geometry layout (as NeRF-based methods do) is often inadequate to capture the *continuous* texture variance in the reference image. This "appearance-geometry entanglement" makes applying 3DGS to applications that require novel appearance, *i.e.* stylization, challenging. For 3DGS, how to properly control and edit the appearance without distorting the original geometry remains under-explored.

In this paper, we present a novel reference-based scene stylization method using 3DGS, dubbed ReGS, to enable real-time stylized view synthesis with high-fidelity textures well-aligned with the given reference. Similar to previous methods, our approach starts with a pretrained 3D Gaussian model of the target scene. The core enabler of ReGS is a novel texture-guided control procedure that makes high-fidelity appearance editing with ease. In particular, we adaptively adjust the local arrangement of responsible Gaussians in the appearance underfitting regions to a state that the desired textures specified in the reference image can be faithfully expressed. The control process is designed to (**1**) automatically identify target local Gaussians using texture clues, and (**2**) structurally distribute tiny Gaussians for fast detail infilling while (**3**) sticking to the original scene structure via a depth-based regularization. With these novel designs, ReGS is able to learn consistent 3D appearance that accurately follows the given reference image.

Following [10], we train ReGS on a set of pseudo-stylized images for view consistency, which are synthetic multi-view data created using extracted scene depth, alongside with a template-based matching loss to ensure style spread to the occluded regions. By combining these techniques with the proposed texture-guided control, ReGS is capable of producing visually appealing stylization results that attain both geometric and perceptual consistency. Through extensive experiments, we demonstrate that ReGS achieves state-of-the-art visual quality compared to existing stylization methods while enabling real-time view synthesis by embracing the fast rendering speed of Gaussian Splatting.

2 Related Work

2.1 3D Scene Representation

Neural Radiance Field. Reconstructing 3D scene from multi-view collections is a long-standing problem in computer vision. Early approaches adopting explicit mesh [22, 23, 24, 25] or voxel [26,

27, 28] based representations often suffer from geometry error and lack of appearance details [29]. Recent methods [30, 31, 32, 33, 34, 35] adopt learnable radiance fields [14] to capture 3D scene implicitly and outperform previous techniques by a large margin. However, NeRF models require millions of network queries for a single rendition that can be extremely time and resource-consuming. To reduce the training time, advanced methods adopt explicit/hybrid representations including voxel grid [18, 16, 15, 36, 37], octree [38, 39, 40], planes [41, 42, 17, 43] and hash grid [20], and successfully reduce the training time from days to minutes. Nevertheless, the rendering speed at inference time is still limited by their volumetric nature, which requires dense sampling along a ray to generate a single pixel.

3D Gaussian Splatting. Recently, 3D Gaussian Splatting (3DGS) [11] achieves real-time novel view synthesis based on a differentiable rasterizer [21] that efficiently projects millions of 3D Gaussians to a 2D canvas. Given its high efficiency, 3DGS becomes a promising solution to enable real-time vision applications, such as human avatar [44, 45, 46, 47], 3D object and immersive scene creation [48, 49, 50, 51], relighting [52, 53, 54, 55], surface or mesh reconstruction [56, 57], 3D segmentation [58, 59, 60], and SLAM [61, 62, 63]. Motivated by its high efficiency, our work explores 3DGS to enable real-time stylized view navigation.

2.2   2D Stylization

Arbitrary Style Transfer. Our method is related to the general 2D stylization [64], which transfers the style from an artwork to a target image while maintaining the original content structure. In the pioneering work, Gatys *et al*. [65] introduce an iterative scheme that progressively reduces the difference between the Gram statistics of generated image and style image features, yet lengthy optimization is required per style. To improve efficiency, later methods [66, 67, 68, 69, 70] focus on arbitrary image/video stylization by transferring the content image to target style spaces in a zero-shot manner. For example, Huang *et al*. [67] introduce AdaIN, which achieves real-time stylization by matching content features with the mean and standard deviation of style features. Linear style transfer [66] instead predicts a linear transformation matrix based on both content and style pairs. For video stylization, it is crucial to maintain temporal coherence of the stylized frames. Techniques [71, 72, 73, 74, 75, 76], such as flow-based wrapping [72], global SSIM constraint [75], and inter-frame feature similarity [76], are proposed to ensure the consistency.

Optimization-based Style Transfer. While arbitrary style transfer is desirable in terms of flexibility, they often fall short of reproducing small stylistic patterns and lack high-frequency details [8, 77]. Optimization-based Stylization [78, 79, 80, 81, 82, 77] is still the primary choice to ensure visual quality. For instance, a coarse-to-fine strategy is proposed by Liao *et al*. [82] to compute the nearest-neighbor field and build a semantically meaningful mapping between input and style images for visual attribute transfer. Kolkin *et al*. [77] reach state-of-the-art stylization quality by replacing the content features with the nearest style feature. To enable better controllability, example-based methods [83, 84, 85, 86] perform wrapping or stylizing based on the aligned correspondences between the style reference and content images. However, their 2D alignment is generally unsuitable for 3D scenes due to occlusions, leading to flickering effects [10].

2.3   3D Stylization

3D scene stylization extends artistic works beyond the 2D canvas [87]. Early works [1, 2] typically back-project image colors as 3D point cloud for processing, and project stylized point features back to 2D for view synthesis. Yet, using point cloud often fails to represent complicated geometry and produces artifacts for complex scenes [8].

Benefiting from NeRF, methods stylizing radiance fields [9, 8, 3, 4, 5, 6, 7] have shown visually compelling and geometry-consistent results than previously possible. Similar to image stylization, several works [9, 3, 6, 7] deal with arbitrary or multiple style transfer using various techniques such as 2D-3D mutual learning [3], deferred style transformation [9], and hypernetwork [6]. While a universal stylizer might be desirable, these methods can only transfer the overall color tone and lack detailed style patterns, *i.e.* brushstrokes. Per-style optimization is still required for better visual quality. Among these methods [4, 8, 5, 88], ARF [8] shows state-of-the-art stylization capability by progressively matching the generated features with the closest style feature via nearest neighbor search. However, these methods are designed for transferring styles from an arbitrary reference and
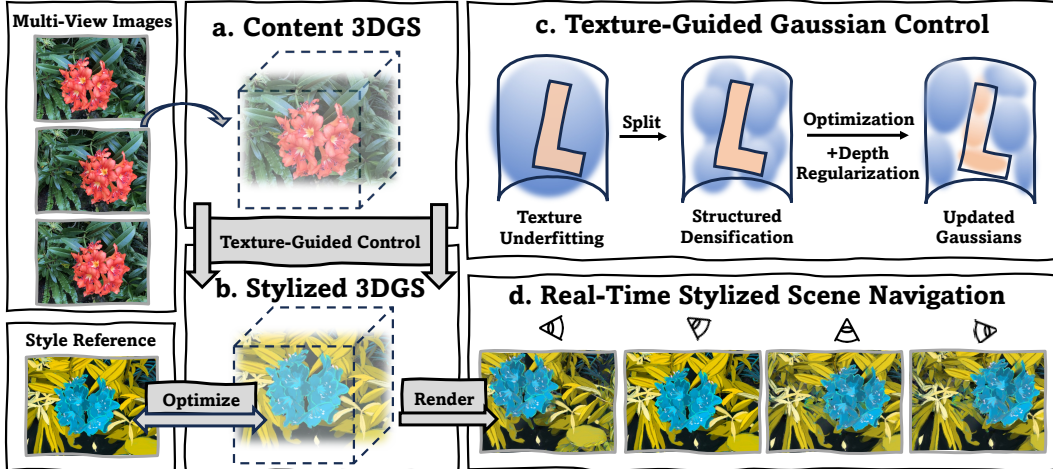
Figure 2: **An overview of ReGS**. (a) The proposed method starts with a pretrained content 3DGS of the target scene, and (b) outputs a stylized 3DGS that follows the reference. (c) We propose Texture-Guided Gaussian Control that can progressively resolve texture underfitting by automatically locating responsible Gaussians and adjusting local geometry layout for fitting high-frequency textures. (d) Once training is done, our method enables real-time stylized scene navigation.

lack controllability over generated results. To this end, Ref-NPR [10] introduces a reference-based scheme that controls stylized appearance based on a content-aligned reference image. Our work also focuses on this setting.

3 Method

An overview of ReGS is shown in Figure 2. ReGS takes a pretrained 3DGS model (Figure 2 (a)) of the target scene as well as a content-aligned reference image as inputs. It outputs a stylized 3DGS model (Figure 2 (b)) that bakes the texture of the reference image into the scene and enables real-time stylized views synthesis (Figure 2 (d)).

As 3DGS represents a scene as discrete Gaussians, simply optimizing its appearance often cannot capture the continuous texture details in the reference image. We introduce a texture-guided control mechanism to progressively address this challenge (Sec. 3.2). To ensure no geometry distortion happens during optimization, we propose a geometry regularization using scene depth (Sec. 3.3). We then introduce two techniques to encourage perceptual-consistent renditions (Sec. 3.4). Finally, we describe our training objectives in Sec. 3.5.

3.1 Preliminary: 3D Gaussian Splatting

Before introducing our method, we first provide a brief review of 3D Gaussian Splatting [11]. 3DGS represents the scene explicitly by a collection of learnable Gaussians. Each 3D Gaussian is attributed by a positional vector $\mu \in \mathbb{R}^3$ and a 3D covariance matrix $\Sigma \in \mathbb{R}^{3 \times 3}$. Its influence on a space point $\mathbf{x}$ is proportional to a Gaussian distribution:

$$G(\mathbf{x}) = e^{-\frac{1}{2}(\mathbf{x}-\mu)^\top \Sigma^{-1}(\mathbf{x}-\mu)}. \tag{1}$$

By definition, the covariance matrix should be positive semi-definite. This is achieved by decomposing Σ into a scaling matrix $\mathbf{S}$ and a quaternion $\mathbf{R}$ *i.e.* $\Sigma = \mathbf{R}\mathbf{S}\mathbf{S}^\top\mathbf{R}^\top$. Each Gaussian also stores an opacity value α_i and a view-dependent color represented by Spherical Harmonic (SH) coefficients.

The rendering procedure is implemented as splatting-based rasterization [21] which projects Gaussians to a 2D canvas. The projected 2D splats are then sorted based on the depth to the camera. After sorting, the final color for each pixel is computed through α-blending:

$$C = \sum_{i=1}^{n} c_i \alpha_i' \prod_{j=1}^{i-1} (1 - \alpha_j'), \tag{2}$$

Style Reference	Stylized Pseudo Views via Depth-based Warping

(a) Rendered depth images   (b) Synthesized pseudo views

Figure 3: Examples of (a) rendered depth maps using Eq.3 and (b) synthesized stylized pseudo views.

where c_i is a view-dependent color of the i-th Gaussian computed from SH. α'_i is the multiplication result of the learned opacity α_i and evaluated value of the projected 2D Gaussian.

During optimization, heuristic controls are employed to adaptively manage the density of Gaussians to better represent the scene. Specifically, it densifies Gaussians with large positional gradients to capture missing geometry and prunes Gaussians with small opacity to improve compactness.

3.2 Texture-Guided Gaussian Control

As a discrete scene representation, the geometry layout and arrangement of Gaussians essentially limit the range of appearance it can express. For example, as shown in Figure 2 (c), appearance underfitting happens frequently at the area where local granularity of Gaussians is greater than the variance of the texture, *e.g.* a smooth colored surface in the original scene is painted with rich details in the reference view. ReGS addresses such challenges via a novel texture-guided control that splits these responsible local Gaussians into a denser set suitable for high-frequency texture. Specifically, the proposed mechanism automatically identifies responsible Gaussians using texture clues and structurally replaces them with a denser set of tiny Gaussians to compensate for the missing details. We describe important designs of the proposed algorithm below.

Texture Guidance. The control algorithm is directly guided by texture clues. Specifically, we accumulate color gradients of all Gaussians over iterations and select Gaussians with larger gradient magnitude than a threshold for densification. We found that a larger color gradient corresponds to Gaussians that have large texture errors while the optimization struggles to find the correct colors to reduce the loss. This control scheme shares a similar spirit with the original control scheme in 3DGS, where they leverage positional gradients to locate Gaussians responsible for missing geometric features. But in stylization, scene geometry is already well-reconstructed through pretraining, and therefore, the positional gradient is no longer informative. As demonstrated in Figure 5, our color-based control scheme is more sensitive for pinpointing Gaussians with missing textures than the positional-based solution. In practical implementation, we increase density based on the gradient statistics of every 100 iterations.

Structured Densification. Traditional mesh subdivision [89] cuts large faces into more sub-faces to express surface details. Sharing a similar spirit, we structurally split each responsible Gaussians into a structured denser set to better represent texture details. Intuitively, after densification, newly added Gaussians need to approximate the original space coverage to avoid inducing large geometry errors, and they should be sufficiently small and form a dense set to capture appearance variance. Based on these considerations, we propose a structured densification scheme that adds tiny Gaussians into the most representative locations surrounding their parent Gaussian. Specifically, we use nine tiny Gaussians to replace a parent Gaussian. Eight of them correspond to eight separate octants divided by the equatorial plane and perpendicular meridian planes of the original ellipsoid. And the rest is placed at the original center. We reduce their size by shrinking the scales with a factor of 8 and copy remaining parameters from their parent Gaussian. We empirically found this setup can roughly maintain a space coverage that approximates the original geometry. As optimization continues, the densified Gaussians are progressively updated to infill missing textures.

3.3 Depth-based Geometry Regularization

While our control mechanism progressively improves texture details, it is essential to ensure the original scene geometry is preserved after optimization. We resort to the scene depth as an additional regularization to penalize geometry changes. Examples of rendered depth are shown in Figure 3 (a).

Formally, we derive the scene depth via a α-blending-based equation:

$$d = \sum_{i=1}^{n} d_i \alpha_i' \prod_{j=1}^{i-1}(1 - \alpha_j'), \tag{3}$$

where the d_i is the z-buffer associated with the ith Gaussian and α_i' is the same evaluated opacity in Eq. 2. d_i is computed by projecting the 3D location μ to the camera space.

The depth regularization is defined as the L_1 distance between a depth image D_i rendered from original scene model $\mathbf{m}$ and a depth image $\widehat{D}_i$ rendered from the stylized model $\widehat{\mathbf{m}}$ using the same camera pose ϕ_i *i.e.* $\mathcal{L}_{depth} = \|\widehat{D}_i - D_i\|_1$.

3.4 View-Consistent Stylization

For stylization, it is necessary to ensure the stylized appearance is consistent across different viewpoints and inpaints the occluded areas. Following [10], we adopt two strategies to address them.

Stylized Pseudo View Supervision. An image with paired depth contains sufficient information to re-render from nearby viewpoints [90]. This allows us to create a set of stylized pseudo views for obtaining additional supervision from the reference image. Our synthesis approach is very similar to classic depth-based 3D warping [90, 91]. Specifically, we back-project the reference image S_R to the world space using the depth image D_R and its camera pose ϕ_R. Then, we re-project these 3D points back to a new viewpoint ϕ_i. The resulting 2D image S_i is used as an additional style supervision. Examples of the created pseudo views are shown in Figure 3 (b). It is important to make sure supervision only happens on meaningful pixels, *i.e.* they are projections of 3D points that are visible from the current viewpoint ϕ_i. Therefore, we conduct a visibility check by comparing the depth between the 2D projections of the 3D points and the depth image D_i from the current viewpoint ϕ_i. This results in a visibility mask M_i. Given the pseudo views and visibility masks, one can define a pseudo view supervision loss as

$$\mathcal{L}_{view} = \frac{1}{\|M_i\|_0}\|M_i\widehat{S}_i - M_iS_i\|_1, \tag{4}$$

where $\|.\|_0$ is the ℓ_0-norm that counts the number of valid pixels and $\widehat{S}_i$ is renderings of the stylized model $\widehat{\mathbf{m}}$.

Template Correspondence Matching (TCM) Loss. To ensure stylized appearance spreads to the occluded areas, we adopt the same TCM loss proposed in [10]. We briefly describe it here and refer readers to [10] for more details. TCM regularizes the difference of semantic correspondences before and after stylization. Given the style reference S_R, its corresponding view I_R, and a scene image I_i rendered from a camera pose ϕ_i, it constructs a guidance feature F_G by $F_{G_i}^{(x,y)} = F_{S_R}^{(x^*,y^*)}$ where

$$(x^*, y^*) = \underset{x',y'}{\arg\min} \; \mathbf{dist}(F_{I_i}^{(x,y)}, F_{I_R}^{(x',y')}). \tag{5}$$

Here, $F_{S_R}, F_{I_R}, F_{I_i}$ denote deep semantic features of image S_R I_R, and I_i extracted by an ImageNet pretrained VGG [92]. **dist** denotes the cosine distance. After obtaining the guidance feature, TCM loss is defined as a cosine distance loss:

$$\mathcal{L}_{TCM} = \mathbf{dist}(F_{\widehat{s}_i}, F_{G_i}), \tag{6}$$

where $F_{\widehat{s}_i}$ is the extracted VGG features of the generated stylized view $\widehat{S}_i$.

3.5 Training Objectives

Besides aforementioned depth loss $\mathcal{L}_{depth}$, pseudo view supervision loss $\mathcal{L}_{view}$ and TCM loss $\mathcal{L}_{TCM}$, ReGS further optimizes a reconstruction loss $\mathcal{L}_{rec}$ and a coarse color-matching loss $\mathcal{L}_{color}$ [10]. The reconstruction loss is defined as the L_1 distance between the reference S_R and the corresponding stylized output $\hat{S}_R$ to enforce appearance baking. The color-matching loss is defined as

$$\mathcal{L}_{color} = \|\widehat{S}_i^{(x,y)} - S_R^{(x^*,y^*)}\|_2^2, \tag{7}$$

where $S^{(x,y)}$ denotes the average color of a patch associated with feature-level index (x,y). Feature-level index is computed using Eq. 5. This loss is directly adapted from [10] to encourage overall
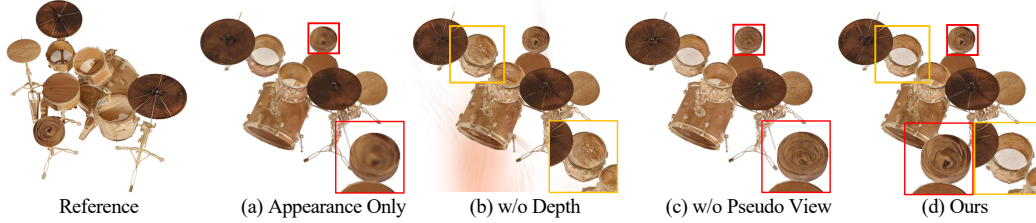
Figure 4: **Ablation study on different components of ReGS**. (a) Optimizing only the appearance of a 3DGS model cannot reproduce texture details. (b) Removing depth regularization causes Gaussians to float out from the surface and distort the origin geometry. (c) Without pseudo-view supervision, results lack view consistency. (d) Our full model produces the best results that faithfully respect the texture in the reference.

color matching in the occluded area. The overall loss for ReGS can be expressed as

$$\mathcal{L} = \lambda_{rec}\mathcal{L}_{rec} + \lambda_{depth}\mathcal{L}_{depth} + \lambda_{view}\mathcal{L}_{view} + \lambda_{tcm}\mathcal{L}_{TCM} + \lambda_{color}\mathcal{L}_{color} \tag{8}$$

where $\lambda_{(.)}$ denotes the balancing parameter.

3.6 Implementation and Training Details

ReGS uses 3D Gaussians [11] as the scene representation and is built upon their official codebase. We follow the default parameter settings to obtain the pretrained 3D Gaussian model of the photo-realistic scene. For stylization, as we do not expect view-dependent effects, we discard the higher order SH and only render diffuse color in the stylization phase. Therefore, content images used in $\mathcal{L}_{TCM}$ and $\mathcal{L}_{color}$ are the results of this diffuse model.

For texture-guided control, we start accumulating gradients after a warm-up of 100 iterations and then perform the densification operation based on the color gradient statistics of every 100 iterations. The control process stops when it reaches half of the total iterations. The gradient threshold is empirically set to $1e - 5$ at the beginning, and we linearly reduce it to $5e - 6$ to allow for refining tiny details in the later training stage. Following [10, 8], we use the ImageNet pretrained VGG16 [92] as the feature extractor and use the features produced by *relu_3* and *relu_4* in $\mathcal{L}_{TCM}$. For balancing parameters we set $\lambda_{rec} = \lambda_{tcm} = 1$, $\lambda_{depth} = 10$, $\lambda_{view} = 2$, and $\lambda_{color} = 15$. At each iteration, we always sample two views: the reference view and a random view. We train our model for 3000 iterations. The proposed method is implemented using PyTorch and trained on one A5000 GPU.

4 Experiments

In this section, we demonstrate the stylization quality and our designs through extensive experiments. **More experiment results and ablation** can be found in the supplemental file and accompanied video.

4.1 Datasets

The only available reference-based stylization dataset is provided by [10]. The dataset contains 12 selected scenes from Blender [14], LLFF [93], and Tanks and Temples [94]. Each scene is paired with a content-aligned reference image.

4.2 Ablation Study

We conduct controlled experiments to analyze the effectiveness of each design choice in ReGS. Results are illustrated in Figures 4 & 5. As illustrated in Figure 4, replacing any components of ReGS will harm the stylization quality. For example, Figure 4 (a) shows that optimizing only the appearance with fixed geometry arrangement like previous methods [8, 6, 3, 9, 10] do fails to recover the texture details. As shown in Figure 4 (b), after removing depth regularization, Gaussians float out from the surface and distort the original scene geometry. Similarly, discarding the pseudo view supervision will induce view-inconsistency as highlighted in the inset (Figure 4 (c)). The full model overcomes these issues and produces more visually appealing results that follow the given reference.
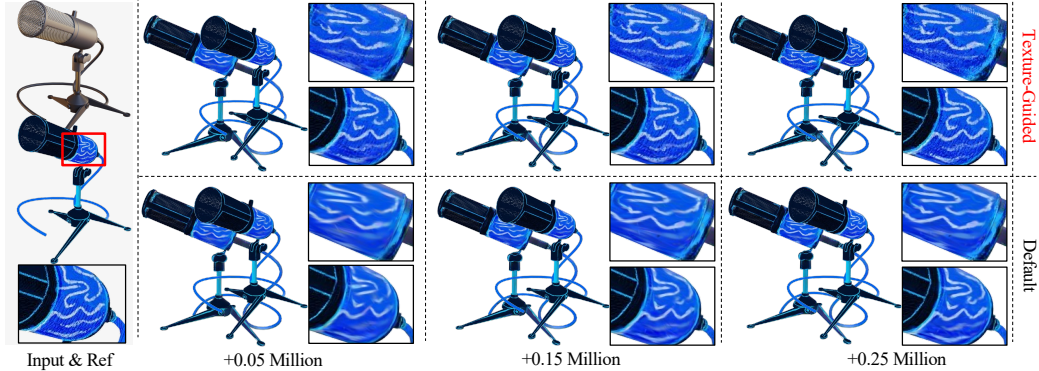
Figure 5: **Effectiveness of Texture-Guided Control.** We conduct controlled experiments by limiting the number of newly densified Gaussians throughout optimization. The pretrained model contains 0.3M Gaussians. The proposed texture-guided control can more faithfully reproduce the target texture details with a small number of Gaussians added (0.05M). The default strategy struggles to capture high-frequency details, even with a large number of Gaussians added (0.25M).

Effectiveness of Texture-Guided Control. The core enabler of ReGS is the proposed texture-guided control mechanism that makes high-fidelity appearance editing with ease. Here, we demonstrate its effectiveness by comparing it with the default positional-gradient-guided density control [11] in addressing texture underfitting. Specifically, we conduct controlled experiments by setting a series of limits on the total number of Gaussians that can grow throughout optimization. Results are reported in Figure 5. One can see that by growing a very small amount of Gaussians (0.05M), the proposed texture-guided method can quickly infill most of the missing details. With more Gaussians added, it can further faithfully reproduce the given texture. In contrast, even with a large amount of new Gaussians (0.25M) created, the default method can barely capture high-frequency texture details. This is mainly because positional gradient is not sensitive to texture errors. As such, it fails to grow Gaussians in the regions with texture underfitting. And further moving these incorrectly placed Gaussians to the correct place for texture infilling is challenging. These results demonstrate our method is indeed more favorable for addressing appearance underfitting. **Study on structured densification can be found in the supplement.**

Table 1: Quantitative comparison of different stylization methods.

Metric	ARF [8]	SNeRF [4]	Ref-NPR [10]	ReGS (Ours)
Ref-LPIPS↓	0.394	0.405	0.339	**0.202**
Robustness↑	26.34	26.03	28.11	**31.27**
Speed (fps)	16.5	16.3	16.4	**91.4**

4.3 Compare with State-of-the-art Methods

To evaluate stylization performance, we compare our method with three state-of-the-art baselines: ARF [8], SNeRF [4], and Ref-NPR [10]. ARF [8] and SNeRF [4] are general stylization methods that conduct style transfer without considering content correspondence. Ref-NPR [10] is a reference-based stylization method similar to ours that aims to precisely edit the 3D appearance based on the reference. All baselines are NeRF-based approaches built upon Plenoxels [15].

Qualitative Evaluation. We report qualitative results in Figure 6. As shown, ARF [8] and SNeRF [4] cannot generate semantic-consistent results with respect to the reference image as they ignore content correspondence. In contrast, Ref-NPR [10] produces more controllable results but yields artifacts. In some challenging cases (*e.g.* last row in Figure 6), it also fails to achieve semantic consistent stylization (*i.e.* green tree in the reference image is colored as white). In contrast, our method achieves better results that reproduce the desired texture, including challenging high-frequency ones.

Quantitative Evaluation. We present quantitative results in Table 1. Results are averaged over all scenes. We follow the protocol from [10] and report Ref-LPIPS and Robustness. Ref-LPIPS computes LPIPS [95] score between the reference image and the 10 nearest test views. To calculate robustness, we first (1) train a stylized base model m_b and use it to render a set of stylized views
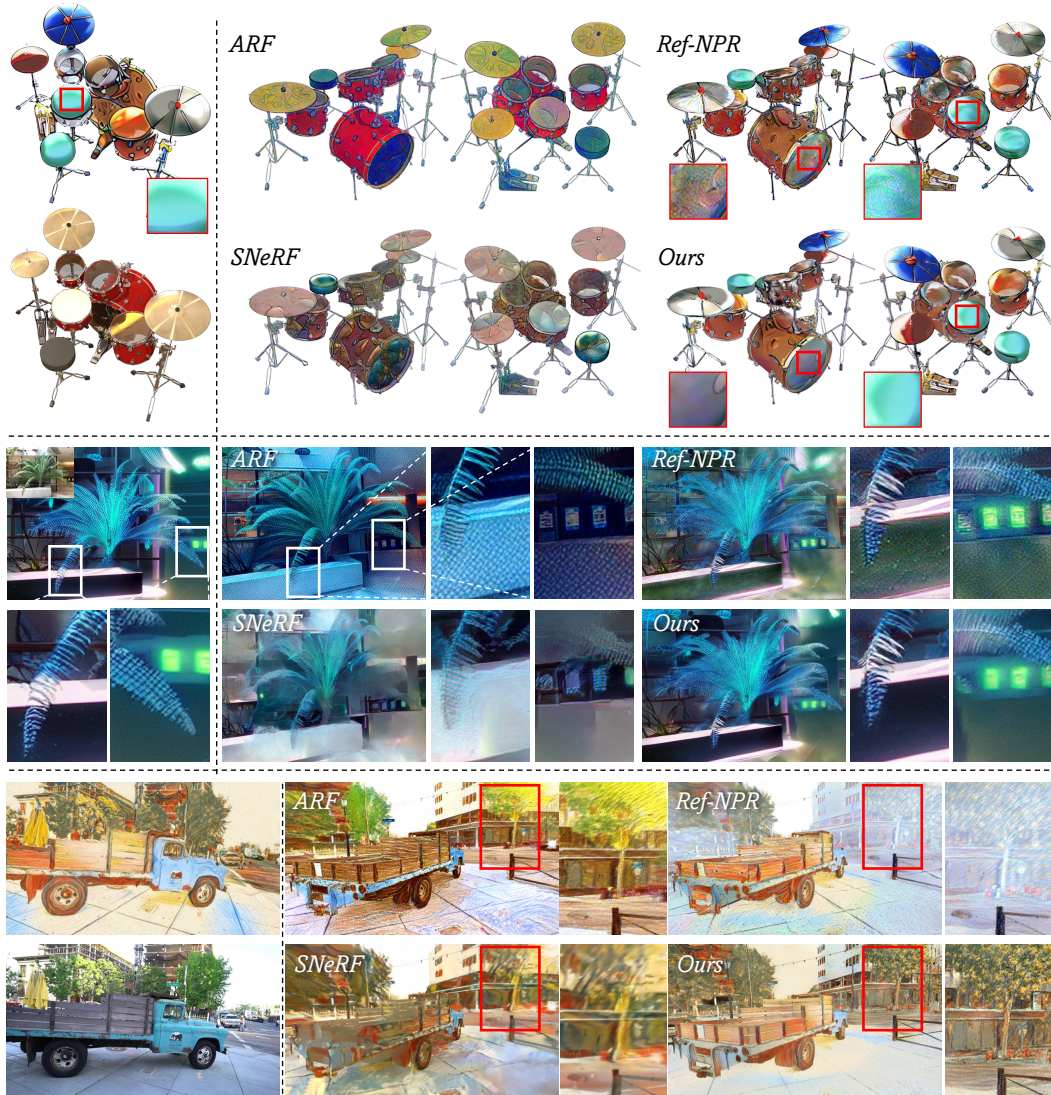
Figure 6: **Visual comparisons with state-of-the-art methods.** Paired reference and content view are shown on the left. Our method produces visual-compelling results that precisely follow the texture of the given reference, including the challenging high-frequency details such as the leaf in the second example. Baseline methods [10, 8, 4] either lack semantic consistency or produce artifacts.

as new references; (2) then we use these references to train another set of stylized models and (3) compute PSNR results between images produced by them and m_b (using the same camera path). To measure run-time efficiency, we also report run-time FPS on a single A5000 GPU. As shown in Table 1, our method achieves the best results in terms of both quality and efficiency. Notably, our method enables real-time stylized view synthesis at 91 FPS.

5 Conclusion

In this work, we introduce ReGS, which adapts Gaussian Splatting for reference-based controllable scene stylization. ReGS adopts a novel texture-guided control mechanism to make high-fidelity appearance editing with ease. This is achieved by adaptively replacing responsible Gaussians with a denser set to express the desired appearance details. The control process is guided by texture clues for appearance editing while preserving original scene geometry through a depth-based regularization. We demonstrate the state-of-the-art scene stylization quality and effective designs of ReGS through extensive experiments. Benefiting from the high efficiency of 3DGS, our method naturally enables real-time stylized view synthesis. Discussions of limitations can be found in the supplemental file.

References

[1] Hsin-Ping Huang, Hung-Yu Tseng, Saurabh Saini, Maneesh Singh, and Ming-Hsuan Yang. Learning to stylize novel views. In *ICCV*, pages 13869–13878, 2021.

[2] Fangzhou Mu, Jian Wang, Yicheng Wu, and Yin Li. 3d photo stylization: Learning to generate stylized novel views from a single image. In *CVPR*, pages 16273–16282, 2022.

[3] Yi-Hua Huang, Yue He, Yu-Jie Yuan, Yu-Kun Lai, and Lin Gao. Stylizednerf: consistent 3d scene stylization as stylized nerf via 2d-3d mutual learning. In *CVPR*, pages 18342–18352, 2022.

[4] Thu Nguyen-Phuoc, Feng Liu, and Lei Xiao. Snerf: stylized neural implicit representations for 3d scenes. *ACM Transactions on Graphics (TOG)*, 41(4):1–11, 2022.

[5] Can Wang, Ruixiang Jiang, Menglei Chai, Mingming He, Dongdong Chen, and Jing Liao. Nerf-art: Text-driven neural radiance fields stylization. *IEEE Transactions on Visualization and Computer Graphics*, 2023.

[6] Pei-Ze Chiang, Meng-Shiun Tsai, Hung-Yu Tseng, Wei-Sheng Lai, and Wei-Chen Chiu. Stylizing 3d scene via implicit representation and hypernetwork. In *WACV*, pages 1475–1484, 2022.

[7] Zhiwen Fan, Yifan Jiang, Peihao Wang, Xinyu Gong, Dejia Xu, and Zhangyang Wang. Unified implicit neural stylization. In *ECCV*, pages 636–654. Springer, 2022.

[8] Kai Zhang, Nick Kolkin, Sai Bi, Fujun Luan, Zexiang Xu, Eli Shechtman, and Noah Snavely. Arf: Artistic radiance fields. In *ECCV*, pages 717–733. Springer, 2022.

[9] Kunhao Liu, Fangneng Zhan, Yiwen Chen, Jiahui Zhang, Yingchen Yu, Abdulmotaleb El Saddik, Shijian Lu, and Eric P Xing. Stylerf: Zero-shot 3d style transfer of neural radiance fields. In *CVPR*, pages 8338–8348, 2023.

[10] Yuechen Zhang, Zexin He, Jinbo Xing, Xufeng Yao, and Jiaya Jia. Ref-npr: Reference-based non-photorealistic radiance fields for controllable scene stylization. In *CVPR*, pages 4242–4251, 2023.

[11] Bernhard Kerbl, Georgios Kopanas, Thomas Leimkühler, and George Drettakis. 3d gaussian splatting for real-time radiance field rendering. *ACM Transactions on Graphics (ToG)*, 42(4):1–14, 2023.

[12] Lukas Höllein, Justin Johnson, and Matthias Nießner. Stylemesh: Style transfer for indoor 3d scene reconstructions. In *CVPR*, pages 6198–6208, 2022.

[13] Jakub Fišer, Ondřej Jamriška, Michal Lukáč, Eli Shechtman, Paul Asente, Jingwan Lu, and Daniel Sỳkora. Stylit: illumination-guided example-based stylization of 3d renderings. *ACM Transactions on Graphics (TOG)*, 35(4):1–11, 2016.

[14] Ben Mildenhall, Pratul P Srinivasan, Matthew Tancik, Jonathan T Barron, Ravi Ramamoorthi, and Ren Ng. Nerf: Representing scenes as neural radiance fields for view synthesis. *Communications of the ACM*, 65(1):99–106, 2021.

[15] Sara Fridovich-Keil, Alex Yu, Matthew Tancik, Qinhong Chen, Benjamin Recht, and Angjoo Kanazawa. Plenoxels: Radiance fields without neural networks. In *CVPR*, pages 5501–5510, 2022.

[16] Cheng Sun, Min Sun, and Hwann-Tzong Chen. Direct voxel grid optimization: Super-fast convergence for radiance fields reconstruction. In *CVPR*, pages 5459–5469, 2022.

[17] Anpei Chen, Zexiang Xu, Andreas Geiger, Jingyi Yu, and Hao Su. Tensorf: Tensorial radiance fields. In *ECCV*, pages 333–350. Springer, 2022.

[18] Lingjie Liu, Jiatao Gu, Kyaw Zaw Lin, Tat-Seng Chua, and Christian Theobalt. Neural sparse voxel fields. *Advances in Neural Information Processing Systems*, 33:15651–15663, 2020.

[19] David B Lindell, Julien NP Martel, and Gordon Wetzstein. Autoint: Automatic integration for fast neural volume rendering. In *CVPR*, pages 14556–14565, 2021.

[20] Thomas Müller, Alex Evans, Christoph Schied, and Alexander Keller. Instant neural graphics primitives with a multiresolution hash encoding. *ACM Transactions on Graphics (ToG)*, 41(4):1–15, 2022.

[21] Matthias Zwicker, Hanspeter Pfister, Jeroen Van Baar, and Markus Gross. Ewa volume splatting. In *Proceedings Visualization, 2001. VIS'01.*, pages 29–538. IEEE, 2001.

[22] Michael Waechter, Nils Moehrle, and Michael Goesele. Let there be color! large-scale texturing of 3d reconstructions. In *ECCV*, pages 836–850. Springer, 2014.

[23] PE DEBEC. Modeling and rendering architecture from photographs: A hybrid geometry-and image-based approach. In *Proc. SIGGRAPH'96*, 1996.

[24] Shichen Liu, Tianye Li, Weikai Chen, and Hao Li. Soft rasterizer: A differentiable renderer for image-based 3d reasoning. In *ICCV*, pages 7708–7717, 2019.

[25] Renke Wang, Guimin Que, Shuo Chen, Xiang Li, Jun Li, and Jian Yang. Creative birds: Self-supervised single-view 3d style transfer. In *ICCV*, pages 8775–8784, 2023.

[26] Kiriakos N Kutulakos and Steven M Seitz. A theory of shape by space carving. *International journal of computer vision*, 38:199–218, 2000.

[27] Steven M Seitz and Charles R Dyer. Photorealistic scene reconstruction by voxel coloring. *International Journal of Computer Vision*, 35:151–173, 1999.

[28] Richard Szeliski and Polina Golland. Stereo matching with transparency and matting. In *ICCV*, pages 517–524. IEEE, 1998.

[29] Kyle Gao, Yina Gao, Hongjie He, Dening Lu, Linlin Xu, and Jonathan Li. Nerf: Neural radiance field in 3d vision, a comprehensive review. *arXiv preprint arXiv:2210.00379*, 2022.

[30] Jonathan T Barron, Ben Mildenhall, Matthew Tancik, Peter Hedman, Ricardo Martin-Brualla, and Pratul P Srinivasan. Mip-nerf: A multiscale representation for anti-aliasing neural radiance fields. In *ICCV*, pages 5855–5864, 2021.

[31] Jonathan T Barron, Ben Mildenhall, Dor Verbin, Pratul P Srinivasan, and Peter Hedman. Mip-nerf 360: Unbounded anti-aliased neural radiance fields. In *CVPR*, pages 5470–5479, 2022.

[32] Ricardo Martin-Brualla, Noha Radwan, Mehdi SM Sajjadi, Jonathan T Barron, Alexey Dosovitskiy, and Daniel Duckworth. Nerf in the wild: Neural radiance fields for unconstrained photo collections. In *CVPR*, pages 7210–7219, 2021.

[33] Alex Yu, Vickie Ye, Matthew Tancik, and Angjoo Kanazawa. pixelnerf: Neural radiance fields from one or few images. In *CVPR*, pages 4578–4587, 2021.

[34] Dor Verbin, Peter Hedman, Ben Mildenhall, Todd Zickler, Jonathan T Barron, and Pratul P Srinivasan. Ref-nerf: Structured view-dependent appearance for neural radiance fields. In *CVPR*, pages 5481–5490, 2022.

[35] Xin Huang, Qi Zhang, Ying Feng, Hongdong Li, Xuan Wang, and Qing Wang. Hdr-nerf: High dynamic range neural radiance fields. In *CVPR*, pages 18398–18408, 2022.

[36] Cheng Sun, Min Sun, and Hwann-Tzong Chen. Direct voxel grid optimization: Super-fast convergence for radiance fields reconstruction. In *CVPR*, pages 5459–5469, 2022.

[37] Peter Hedman, Pratul P Srinivasan, Ben Mildenhall, Jonathan T Barron, and Paul Debevec. Baking neural radiance fields for real-time view synthesis. In *ICCV*, pages 5875–5884, 2021.

[38] Alex Yu, Ruilong Li, Matthew Tancik, Hao Li, Ren Ng, and Angjoo Kanazawa. Plenoctrees for real-time rendering of neural radiance fields. In *ICCV*, pages 5752–5761, 2021.

[39] Liao Wang, Jiakai Zhang, Xinhang Liu, Fuqiang Zhao, Yanshun Zhang, Yingliang Zhang, Minye Wu, Jingyi Yu, and Lan Xu. Fourier plenoctrees for dynamic radiance field rendering in real-time. In *CVPR*, pages 13524–13534, 2022.

[40] Haotian Bai, Yiqi Lin, Yize Chen, and Lin Wang. Dynamic plenoctree for adaptive sampling refinement in explicit nerf. In *ICCV*, pages 8785–8795, 2023.

[41] Eric R Chan, Connor Z Lin, Matthew A Chan, Koki Nagano, Boxiao Pan, Shalini De Mello, Orazio Gallo, Leonidas J Guibas, Jonathan Tremblay, Sameh Khamis, et al. Efficient geometry-aware 3d generative adversarial networks. In *CVPR*, pages 16123–16133, 2022.

[42] Ang Cao and Justin Johnson. Hexplane: A fast representation for dynamic scenes. In *CVPR*, pages 130–141, 2023.

[43] Sara Fridovich-Keil, Giacomo Meanti, Frederik Rahbæk Warburg, Benjamin Recht, and Angjoo Kanazawa. K-planes: Explicit radiance fields in space, time, and appearance. In *CVPR*, pages 12479–12488, 2023.

[44] Liangxiao Hu, Hongwen Zhang, Yuxiang Zhang, Boyao Zhou, Boning Liu, Shengping Zhang, and Liqiang Nie. Gaussianavatar: Towards realistic human avatar modeling from a single video via animatable 3d gaussians. *arXiv preprint arXiv:2312.02134*, 2023.

[45] Zhe Li, Zerong Zheng, Lizhen Wang, and Yebin Liu. Animatable gaussians: Learning pose-dependent gaussian maps for high-fidelity human avatar modeling. *arXiv preprint arXiv:2311.16096*, 2023.

[46] Mengtian Li, Shengxiang Yao, Zhifeng Xie, Keyu Chen, and Yu-Gang Jiang. Gaussianbody: Clothed human reconstruction via 3d gaussian splatting. *arXiv preprint arXiv:2401.09720*, 2024.

[47] Muhammed Kocabas, Jen-Hao Rick Chang, James Gabriel, Oncel Tuzel, and Anurag Ranjan. Hugs: Human gaussian splats. *arXiv preprint arXiv:2311.17910*, 2023.

[48] Jiaxiang Tang, Jiawei Ren, Hang Zhou, Ziwei Liu, and Gang Zeng. Dreamgaussian: Generative gaussian splatting for efficient 3d content creation. In *ICLR*, 2024.

[49] Taoran Yi, Jiemin Fang, Guanjun Wu, Lingxi Xie, Xiaopeng Zhang, Wenyu Liu, Qi Tian, and Xinggang Wang. Gaussiandreamer: Fast generation from text to 3d gaussian splatting with point cloud priors. *arXiv preprint arXiv:2310.08529*, 2023.

[50] Jaeyoung Chung, Suyoung Lee, Hyeongjin Nam, Jaerin Lee, and Kyoung Mu Lee. Luciddreamer: Domain-free generation of 3d gaussian splatting scenes. *arXiv preprint arXiv:2311.13384*, 2023.

[51] Xian Liu, Xiaohang Zhan, Jiaxiang Tang, Ying Shan, Gang Zeng, Dahua Lin, Xihui Liu, and Ziwei Liu. Humangaussian: Text-driven 3d human generation with gaussian splatting. *arXiv preprint arXiv:2311.17061*, 2023.

[52] Jian Gao, Chun Gu, Youtian Lin, Hao Zhu, Xun Cao, Li Zhang, and Yao Yao. Relightable 3d gaussian: Real-time point cloud relighting with brdf decomposition and ray tracing. *arXiv preprint arXiv:2311.16043*, 2023.

[53] Shunsuke Saito, Gabriel Schwartz, Tomas Simon, Junxuan Li, and Giljoo Nam. Relightable gaussian codec avatars. *arXiv preprint arXiv:2312.03704*, 2023.

[54] Zhihao Liang, Qi Zhang, Ying Feng, Ying Shan, and Kui Jia. Gs-ir: 3d gaussian splatting for inverse rendering. *arXiv preprint arXiv:2311.16473*, 2023.

[55] Yahao Shi, Yanmin Wu, Chenming Wu, Xing Liu, Chen Zhao, Haocheng Feng, Jingtuo Liu, Liangjun Zhang, Jian Zhang, Bin Zhou, et al. Gir: 3d gaussian inverse rendering for relightable scene factorization. *arXiv preprint arXiv:2312.05133*, 2023.

[56] Antoine Guédon and Vincent Lepetit. Sugar: Surface-aligned gaussian splatting for efficient 3d mesh reconstruction and high-quality mesh rendering. *arXiv preprint arXiv:2311.12775*, 2023.

[57] Hanlin Chen, Chen Li, and Gim Hee Lee. Neusg: Neural implicit surface reconstruction with 3d gaussian splatting guidance. *arXiv preprint arXiv:2312.00846*, 2023.

[58] Shijie Zhou, Haoran Chang, Sicheng Jiang, Zhiwen Fan, Zehao Zhu, Dejia Xu, Pradyumna Chari, Suya You, Zhangyang Wang, and Achuta Kadambi. Feature 3dgs: Supercharging 3d gaussian splatting to enable distilled feature fields. *arXiv preprint arXiv:2312.03203*, 2023.

[59] Jiazhong Cen, Jiemin Fang, Chen Yang, Lingxi Xie, Xiaopeng Zhang, Wei Shen, and Qi Tian. Segment any 3d gaussians. *arXiv preprint arXiv:2312.00860*, 2023.

[60] Bin Dou, Tianyu Zhang, Yongjia Ma, Zhaohui Wang, and Zejian Yuan. Cosseggaussians: Compact and swift scene segmenting 3d gaussians. *arXiv preprint arXiv:2401.05925*, 2024.

[61] Vladimir Yugay, Yue Li, Theo Gevers, and Martin R Oswald. Gaussian-slam: Photo-realistic dense slam with gaussian splatting. *arXiv preprint arXiv:2312.10070*, 2023.

[62] Hidenobu Matsuki, Riku Murai, Paul HJ Kelly, and Andrew J Davison. Gaussian splatting slam. *arXiv preprint arXiv:2312.06741*, 2023.

[63] Mingrui Li, Shuhong Liu, and Heng Zhou. Sgs-slam: Semantic gaussian splatting for neural dense slam. *arXiv preprint arXiv:2402.03246*, 2024.

[64] Yongcheng Jing, Yezhou Yang, Zunlei Feng, Jingwen Ye, Yizhou Yu, and Mingli Song. Neural style transfer: A review. *IEEE transactions on visualization and computer graphics*, 26(11):3365–3385, 2019.

[65] Leon A Gatys, Alexander S Ecker, and Matthias Bethge. Image style transfer using convolutional neural networks. In *CVPR*, pages 2414–2423, 2016.

[66] Xueting Li, Sifei Liu, Jan Kautz, and Ming-Hsuan Yang. Learning linear transformations for fast image and video style transfer. In *CVPR*, pages 3809–3817, 2019.

[67] Xun Huang and Serge Belongie. Arbitrary style transfer in real-time with adaptive instance normalization. In *ICCV*, pages 1501–1510, 2017.

[68] Songhua Liu, Tianwei Lin, Dongliang He, Fu Li, Meiling Wang, Xin Li, Zhengxing Sun, Qian Li, and Errui Ding. Adaattn: Revisit attention mechanism in arbitrary neural style transfer. In *ICCV*, pages 6649–6658, 2021.

[69] Dae Young Park and Kwang Hee Lee. Arbitrary style transfer with style-attentional networks. In *CVPR*, pages 5880–5888, 2019.

[70] Yongcheng Jing, Xiao Liu, Yukang Ding, Xinchao Wang, Errui Ding, Mingli Song, and Shilei Wen. Dynamic instance normalization for arbitrary style transfer. In *Proceedings of the AAAI conference on artificial intelligence*, volume 34, pages 4369–4376, 2020.

[71] Dongdong Chen, Jing Liao, Lu Yuan, Nenghai Yu, and Gang Hua. Coherent online video style transfer. In *ICCV*, pages 1105–1114, 2017.

[72] Haozhi Huang, Hao Wang, Wenhan Luo, Lin Ma, Wenhao Jiang, Xiaolong Zhu, Zhifeng Li, and Wei Liu. Real-time neural style transfer for videos. In *CVPR*, pages 783–791, 2017.

[73] Manuel Ruder, Alexey Dosovitskiy, and Thomas Brox. Artistic style transfer for videos and spherical images. *International Journal of Computer Vision*, 126(11):1199–1219, 2018.

[74] Wenjing Wang, Jizheng Xu, Li Zhang, Yue Wang, and Jiaying Liu. Consistent video style transfer via compound regularization. In *Proceedings of the AAAI conference on artificial intelligence*, volume 34, pages 12233–12240, 2020.

[75] Xinxiao Wu and Jialu Chen. Preserving global and local temporal consistency for arbitrary video style transfer. In *Proceedings of the 28th ACM International Conference on Multimedia*, pages 1791–1799, 2020.

[76] Yingying Deng, Fan Tang, Weiming Dong, Haibin Huang, Chongyang Ma, and Changsheng Xu. Arbitrary video style transfer via multi-channel correlation. In *Proceedings of the AAAI Conference on Artificial Intelligence*, volume 35, pages 1210–1217, 2021.

[77] Nicholas Kolkin, Michal Kucera, Sylvain Paris, Daniel Sykora, Eli Shechtman, and Greg Shakhnarovich. Neural neighbor style transfer. *arXiv e-prints*, pages arXiv–2203, 2022.

[78] Chuan Li and Michael Wand. Combining markov random fields and convolutional neural networks for image synthesis. In *CVPR*, pages 2479–2486, 2016.

[79] Eric Risser, Pierre Wilmot, and Connelly Barnes. Stable and controllable neural texture synthesis and style transfer using histogram losses. *arXiv preprint arXiv:1701.08893*, 2017.

[80] Shuyang Gu, Congliang Chen, Jing Liao, and Lu Yuan. Arbitrary style transfer with deep feature reshuffle. In *CVPR*, pages 8222–8231, 2018.

[81] Nicholas Kolkin, Jason Salavon, and Gregory Shakhnarovich. Style transfer by relaxed optimal transport and self-similarity. In *CVPR*, pages 10051–10060, 2019.

[82] Jing Liao, Yuan Yao, Lu Yuan, Gang Hua, and Sing Bing Kang. Visual atribute transfer through deep image analogy. *ACM Transactions on Graphics*, 36(4):120, 2017.

[83] Ondřej Jamriška, Šárka Sochorová, Ondřej Texler, Michal Lukáč, Jakub Fišer, Jingwan Lu, Eli Shechtman, and Daniel Sỳkora. Stylizing video by example. *ACM Transactions on Graphics (TOG)*, 38(4):1–11, 2019.

[84] Ahmed Selim, Mohamed Elgharib, and Linda Doyle. Painting style transfer for head portraits using convolutional neural networks. *ACM Transactions on Graphics (ToG)*, 35(4):1–18, 2016.

[85] YiChang Shih, Sylvain Paris, Connelly Barnes, William T Freeman, and Frédo Durand. Style transfer for headshot portraits. *ACM Transactions on Graphics*, 33(4):1–14, 2014.

[86] Ondřej Texler, David Futschik, Michal Kučera, Ondřej Jamriška, Šárka Sochorová, Menclei Chai, Sergey Tulyakov, and Daniel Sỳkora. Interactive video stylization using few-shot patch-based training. *ACM Transactions on Graphics (TOG)*, 39(4):73–1, 2020.

[87] Yingshu Chen, Guocheng Shao, Ka Chun Shum, Binh-Son Hua, and Sai-Kit Yeung. Advances in 3d neural stylization: A survey. *arXiv preprint arXiv:2311.18328*, 2023.

[88] Zicheng Zhang, Yinglu Liu, Congying Han, Yingwei Pan, Tiande Guo, and Ting Yao. Transforming radiance field with lipschitz network for photorealistic 3d scene stylization. In *CVPR*, pages 20712–20721, 2023.

[89] Denis Zorin, Peter Schröder, and Wim Sweldens. Interpolating subdivision for meshes with arbitrary topology. In *Proceedings of the 23rd annual conference on Computer graphics and interactive techniques*, pages 189–192, 1996.

[90] William R Mark, Leonard McMillan, and Gary Bishop. Post-rendering 3d warping. In *Proceedings of the 1997 symposium on Interactive 3D graphics*, pages 7–ff, 1997.

[91] Leonard McMillan and Gary Bishop. Plenoptic modeling: An image-based rendering system. In *Seminal Graphics Papers: Pushing the Boundaries, Volume 2*, pages 433–440. 2023.

[92] Karen Simonyan and Andrew Zisserman. Very deep convolutional networks for large-scale image recognition. *arXiv preprint arXiv:1409.1556*, 2014.

[93] Ben Mildenhall, Pratul P Srinivasan, Rodrigo Ortiz-Cayon, Nima Khademi Kalantari, Ravi Ramamoorthi, Ren Ng, and Abhishek Kar. Local light field fusion: Practical view synthesis with prescriptive sampling guidelines. *ACM Transactions on Graphics (TOG)*, 38(4):1–14, 2019.

[94] Arno Knapitsch, Jaesik Park, Qian-Yi Zhou, and Vladlen Koltun. Tanks and temples: Benchmarking large-scale scene reconstruction. *ACM Transactions on Graphics*, 36(4), 2017.

[95] Richard Zhang, Phillip Isola, Alexei A Efros, Eli Shechtman, and Oliver Wang. The unreasonable effectiveness of deep features as a perceptual metric. In *Proceedings of the IEEE conference on computer vision and pattern recognition*, pages 586–595, 2018.